ACADEMIC PRESS

Available online at www.sciencedirect.com
SCIENCE DIRECT®

Journal of Catalysis 216 (2003) 396–405

JOURNAL OF CATALYSIS

www.elsevier.com/locate/jcat

New perspectives on basic zeolites as catalysts and catalyst supports

Robert J. Davis

Department of Chemical Engineering, University of Virginia, 102 Engineers Way, Charlottesville, VA 22904-4741, USA

Received 8 July 2002; revised 4 September 2002; accepted 8 October 2002

Abstract

Zeolites are aluminosilicate molecular sieves that have great potential as basic catalysts and catalyst supports. In particular, this paper discusses recent work and future directions with zeolite X containing exchanged alkali metal cations, occluded alkali metal oxides, and occluded alkali metals. Probe reactions such as alkylation of toluene with methanol, cyclo-addition of carbon dioxide to ethylene oxide, isomerization of 1-butene, and alkylation of toluene with ethylene are catalyzed by the basic X zeolites, depending on the preparation method. Basic zeolites are also excellent supports for nanometer-sized Ru metal clusters used to catalyze the ammonia synthesis reaction. In that case, occluded barium oxide effectively promotes the reaction on Ru-loaded Ba-exchanged zeolite X. These examples illustrate important principles that can be used to guide future design of shape-selective base catalysts.

Keywords: Faujasite; Zeolite X; Cesium; Sodium; Potassium; Alkylation; Isomerization; Cyclo-addition of carbon dioxide; Ammonia synthesis; Iodine, adsorption of; Carbon dioxide, adsorption of

1. Introduction

Tanabe and Hölderich performed a statistical survey of industrial processes using solid acids, solid bases, and acid–base bifunctional catalysts and counted 103, 10, and 14 industrial processes for these types of catalysts, respectively, [1]. Clearly, solid acids have received most of the attention in industrial applications. However, as novel base materials become known and new base-catalyzed reactions are found to be commercially relevant, fundamental studies of solid bases will be necessary for these catalysts to achieve the success of solid acids.

Solid base catalysts exhibit high activities and selectivities for many kinds of reactions, including condensations, alkylations, cyclizations, and isomerizations; however, many of these processes are carried out industrially using liquid bases as catalysts. These applications can require nearly stoichiometric amounts of the liquid base for conversion to the desired product. Replacement of liquid base catalysts with solid base catalysts allows easier separation from the product as well as possible regeneration and reuse. Basic solids also have the added advantages of being noncorrosive and environmentally friendly, which allows easier disposal. Solids that expose both acidic and basic surface sites are called "bifunctional" and represent an exciting new class of catalytic materials.

A molecular-level understanding of solid basicity is required before structure/function properties of new materials can be effectively predicted. A significant fraction of the research on solid bases therefore involves the correlation of base strength to catalyst composition. However, since strong bases are also poisoned by carbon dioxide and water, common side products in catalytic reactions, new base catalysts that are more resistant to deactivation by these molecules need to be developed. The search for novel solid bases that catalyze transformations with high product selectivity, high reaction rate, and low deactivation rate is an ongoing process.

This paper is not intended to be a comprehensive review, but instead focuses on recent aspects of our work dealing with zeolites as basic solids and as basic supports for alkali metals and alkali metal oxides. To the best of our knowledge, an industrial process utilizing a basic zeolite catalyst has not been commercialized. A couple of processes have reached pilot plant scale. For example, Merck and Co. used cesium sulfate impregnated into ZSM-5 as a catalyst for the synthesis of 4-methyl thiazol (Fig. 1a) [2]. Because the reaction was run in the vapor phase (723–773 K) in the presence of water vapor, a zeolite with high hydrothermal stability was chosen. Another example of a basic-zeolite-catalyzed process is the oxyiodination of naphthalene over

E-mail address: rjd4f@virginia.edu.

0021-9517/03/$ – see front matter
doi:10.1016/S0021-9517(02)00034-9

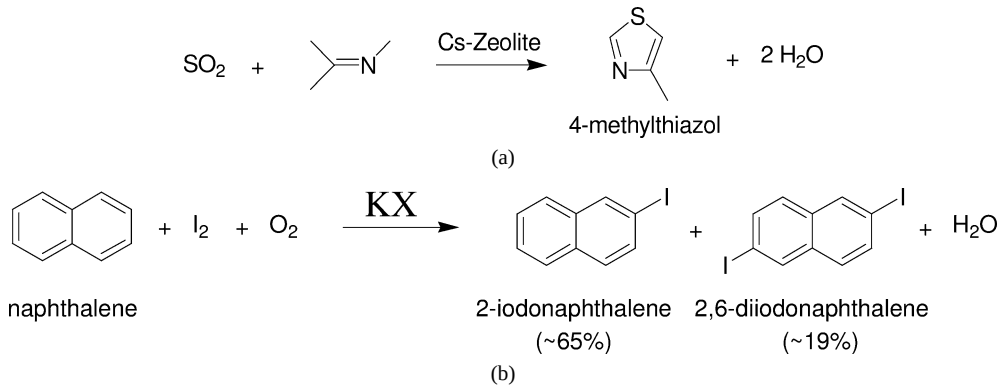

Fig. 1. (a) Synthesis of methylthiazol catalyzed by Cs-loaded ZSM-5. (b) Oxyiodination of naphthalene catalyzed by K-exchanged X zeolite.

potassium-exchanged zeolite X (Fig. 1b) [3]. Researchers at Eastman Chemical Co. suggest that iodine is strongly adsorbed in the basic zeolite, which leads to polarization of the molecule. The resulting product distribution indicates that shape selectivity may be important in this system. In addition to supporting occluded bases, zeolites can also be used as supports for transition metals. Reactions that require base promotion of a catalytic transition metal site are particularly interesting. Our progress with basic zeolite X as a support for Ru metal clusters is also described in this paper.

2. Ion-exchanged zeolites as electron donors

Zeolites are aluminosilicates that are constructed from TO_4 tetrahedra (T = tetrahedral atom, e.g., Si, Al) with each apical oxygen atom shared with an adjacent tetrahedron. When tetrahedra containing Si^{4+} and Al^{3+} are connected to form a three-dimensional zeolite framework, there is a negative charge associated with each Al^{3+} atom. The negative framework charge is balanced by an exchangeable cation, yielding electrical neutrality. Figure 2 illustrates the highly porous nature of faujasite and the need for charge-balancing cations. The examples discussed in this paper focus on zeolite X, a faujasite-type zeolite with a silicon-to-aluminum ratio ranging from 1 to 1.5.

The basicity of ion-exchanged zeolites arises from the framework negative charge. Thus, the relatively high aluminum content of zeolite X results in a substantial framework negative charge, which makes X one of the most basic zeolites when in the alkali-exchanged form. For an excellent discussion of basic zeolites, please see the comprehensive review by Barthomeuf [4].

Finding an appropriate probe molecule to interrogate the basicity of alkali-exchanged zeolites has proved to be problematic. Basic sites in zeolites are commonly characterized by IR spectroscopy coupled with temperature-programmed desorption of adsorbed probe molecules such as carbon dioxide [5–9], pyrrole [10–12], and chloroform [13–15]. A problem with this technique is that many of the commonly used probe molecules decompose or react upon interaction with the basic site and, therefore, do not effectively interrogate the catalyst surface.

To complement IR spectroscopy of probe molecules, we have used UV–vis spectroscopy of adsorbed iodine to probe the basicity of zeolites. A sample with an exposed ionizable electron may act as a Lewis base with respect to I_2 [16]. The use of I_2 as a molecular probe of electron donor strength associated with the gas phase [17–22] and

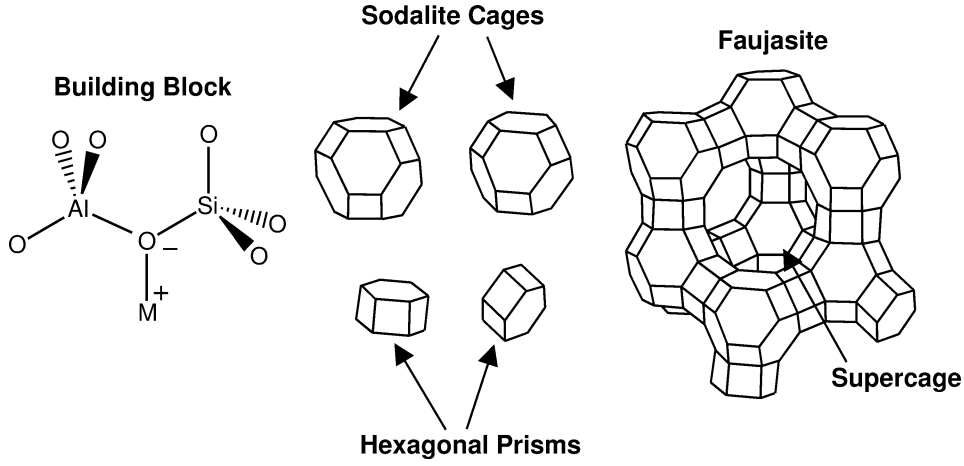

Fig. 2. Schematic diagram of a faujasite-type zeolite. M^+ is a charge-balancing cation.

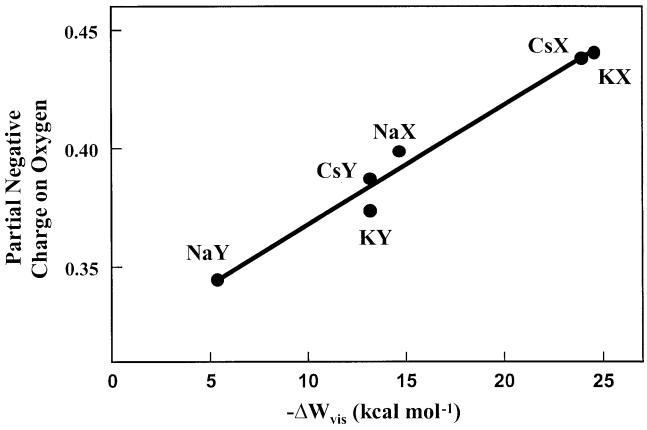

Fig. 3. Partial negative charge on oxygen as a function of energy calculated from the blue shift of adsorbed iodine in relation to gaseous iodine. (Reproduced from E.J. Doskocil, S.V. Bordawekar, B.G. Kay, R.J. Davis, J. Phys. Chem. B 103 (1999) 6277, with permission from the American Chemical Society.)

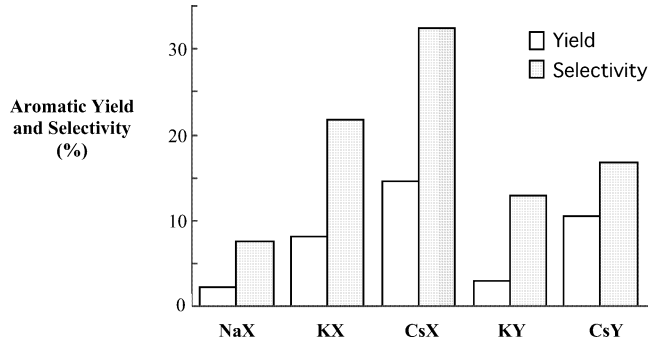

Fig. 4. Toluene alkylation over alkali-exchanged zeolites X and Y. Conditions: w/F: 20–30 g h mol^{-1}; $T = 680$–690 K. Yield is based on the amount of side-chain alkylation products relative to methanol fed. Selectivity is defined as the amount of methanol used to form side-chain alkylation products divided by the total amount of methanol reacted—the only other side product of significance was carbon monoxide resulting from methanol decomposition. (Adapted from W.S. Wieland, R.J. Davis, J.M. Garces, J. Catal. 173 (1998) 490, with permission from Academic Press.)

solvated molecules [16,23–37] has been well documented in the literature. Many researchers have correlated the blue-shift in the visible absorption band of an iodine donor-acceptor complex with its heat of formation [23,25,38].

Mulliken predicted the use of iodine adsorption to probe donor strength of solids [24], and sorption of iodine in zeolites has been investigated in the past [39,40]. Results confirm that iodine interacts with the basic framework oxygen and not the charge-balancing cation [39,40].

Recently, the visible absorption spectrum of iodine has been used to rank the basic strength of the oxygen atoms in various zeolites [41]. Choi et al. have shown that a blue shift occurs in the visible spectrum of adsorbed iodine with increasing electropositivity of the alkali counterion from Li to K, as well as with increasing aluminum content in the zeolite framework [41]. Figure 3 summarizes the basicity ranking of alkali-exchanged X and Y zeolites determined by the blue shift in the UV–vis absorption spectrum of adsorbed iodine [42]. The average partial negative charge of the oxygen atoms in the zeolite framework was estimated from the Sanderson intermediate electronegativity principle. Thus results in Fig. 3 clearly show that Cs- and K-exchanged X zeolites are the most basic samples in the series. One reason that CsX is not more basic than KX is that only a fraction of the cations in zeolite X can be exchanged with Cs, whereas nearly all of the cations can be exchanged with K. In addition, a smaller degree of blue shift of CsX might result from the steric hindrance between I_2 and framework oxygen due to the large size of Cs.

The stabilization of radicals in zeolite pores is also related to the basicity of the framework oxygen atoms. For example, the formation of anion radicals by photoexcitation of pyrene [43,44] and 1,2,4,5-tetracyanobenzene [45] was used to evaluate the electron donor properties of zeolites. In addition, adsorbed methyl viologen [46] and its radical cation formed by photoexcitation [47,48] were used to rank the donor strength of alkali-exchanged zeolites. For a more complete discussion on the photochemistry of molecules adsorbed on zeolites and other solids, please see the review by Thomas [49].

3. Reactivity of ion-exchanged zeolite X

Characterization of ion-exchanged zeolites indicates that they expose solid base sites, especially after exchange with heavy alkali metal cations. Whereas many reactions are catalyzed by ion-exchanged zeolites, one that is particularly interesting over these materials is the side-chain alkylation of toluene with methanol to form styrene and/or ethylbenzene [50–52], with alkali-exchanged zeolites demonstrating the highest activity and selectivity. Figure 4 summarizes the activity and selectivity of the reaction over a range of alkali-exchanged faujasites. (Selectivity in this case is defined as the amount of methanol used to form side-chain alkylation products divided by the total amount of methanol reacted—the only other side product of significance was carbon monoxide resulting from methanol decomposition.) Whereas Cs-exchanged X zeolite is the most effective catalyst represented in Fig. 4, no activity for the reaction was observed over a Cs-doped alumina [52]. In addition, the reaction was promoted further by the addition of boric acid to the Cs-exchanged zeolite, presumably by lowering the decomposition rate of methanol to carbon monoxide [51,52]. Even after addition of boric acid, no side-chain alkylation was observed on Cs-doped alumina. Evidently, the unique environment inside the microporous zeolite is important for this base-catalyzed reaction.

Palomares et al. used in situ infrared spectroscopy to study the reaction over basic catalysts, including magnesia, hydrotalcites, and zeolites [53]. They concluded that the key requirements for the reaction are: (1) sufficient base strength to dehydrogenate methanol into formaldehyde, (2) stabilization of sorbed toluene and polarization of its

methyl group, and (3) balanced sorption stoichiometry of the two reactants. The second and third requirements are achieved in zeolites by interaction of toluene with the exchangeable alkali metal cation. Indeed, CsX was shown to have adequate basicity to activate methanol and a strong heat of toluene adsorption associated with the Cs cations. In a related study of zeolite X, Lee et al. showed that the acceptor strength of alkali metal cations for iodide ions increased with increasing size, with Cs exhibiting the greatest adsorption energy [54]. It is therefore very important to consider both the Lewis *acid* and *base* character of alkali-exchanged zeolites when considering their use in reactions normally thought of as base-catalyzed. This will be a recurring theme throughout this paper.

4. Basic zeolites containing occluded alkali metal oxides

Occlusion of alkali metal oxide clusters in zeolite cages via decomposition of impregnated alkali metal salts results in a further increase in the basicity of these materials [5,55–60]. The supported species are typically introduced through wet impregnation of a solution containing the solvated precursor into the zeolite pores. Calcination decomposes the occluded compounds and creates the supported alkali metal oxides.

The nature of the final occluded alkali species has been elusive, and the actual structure of the occluded oxide is still in question. NMR spectroscopy has been used to study cesium species loaded into zeolites in excess of ion-exchange capacity, but the results were inconclusive [58,61,62]. In addition, a recent NMR study of a variety of bulk alkali metal oxides, superoxides, and peroxides suggests that the peroxide and superoxide phases should be considered for their role in catalytic reactions as both a base and an oxidant [63]. In particular, Krawietz et al. could not successfully prepare bulk phase Cs_2O by conventional chemical methods, whereas stoichiometric lighter alkali metal oxides could be prepared. Their intriguing result suggests the possibility that higher oxides such as cesium peroxide and cesium superoxide might be present in zeolite-supported cesium oxide samples.

Iodine cannot be used as a probe molecule for the basicity of occluded alkali metal oxides since it irreversibly adsorbs and probably decomposes on those samples [42]. We have therefore focused on CO_2 adsorption to probe the basicity of alkali metal oxides occluded in the zeolite pores. Figure 5 shows the differential heat released upon adsorption of CO_2 on Cs-exchanged X zeolite containing various loadings of occluded cesium oxide, denoted as CsO_x/CsX [64]. Most basic sites adsorb CO_2 with an enthalpy of about -100 kJ mol^{-1}. This result is very different than the enthalpy of adsorption associated with bulk "Cs_2O," which was measured to be about -270 kJ mol^{-1}. Thus, the bulk oxide had sites significantly stronger than those in CsO_x/CsX. As mentioned earlier, the commercial bulk "Cs_2O" sample

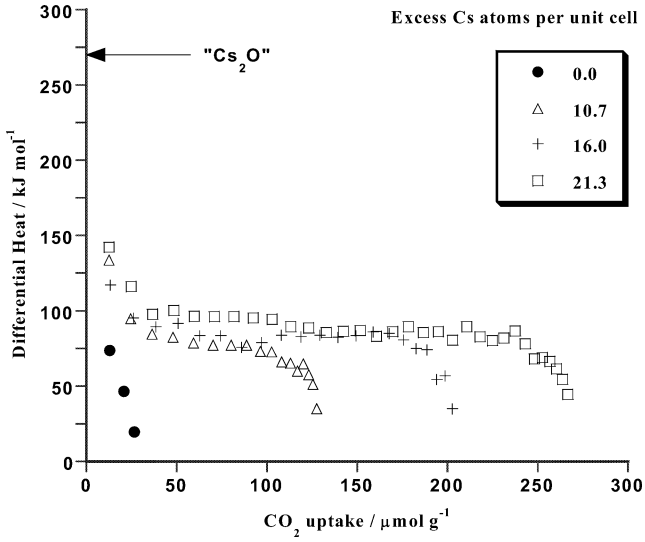

Fig. 5. Differential heats of adsorption (plotted as heat released) as a function of CO_2 uptake for CsO_x/CsX zeolite. For comparison, the initial heat of adsorption on bulk "Cs_2O" is also shown. (Adapted from S.V. Bordawekar, R.J. Davis, J. Catal. 189 (2000) 79, with permission from Academic Press.)

was probably not a pure compound, but may have contained a mixture of cesium suboxides, peroxides, and superoxides with an average formula claimed to be Cs_2O. Nevertheless, after thermal treatment the surfaces of "Cs_2O" were much more basic than those of the occluded alkali metal oxides.

To help us interpret the results from CO_2 adsorption microcalorimetry, we initiated, together with Professor Matthew Neurock, a computational study of CO_2 adsorption on model cesium oxide surfaces. Our goal was to gain some insights into the nature of the cesium oxide occluded in zeolite pores by comparing the energetics of CO_2 adsorption on bulk cesium compounds.

In this study, stoichiometric cesium oxide (Cs_2O), cesium peroxide (Cs_2O_2), and cesium superoxide (CsO_2) were examined. The unit cell for each crystal structure was constructed and the geometry was optimized. Different cuts were made in the superstructure to establish the most favorable surface. A carbon dioxide molecule was then placed on the surface in order to calculate its adsorption strength. The detailed results of the calculations are too lengthy to present here but will be described in a forthcoming paper [65]. The major findings are presented below.

The crystal structure of Cs_2O contains double layers of Cs atoms that, if exposed to the surface, do not adsorb CO_2. Evidently, both oxygen and cesium atoms must be exposed in order to chemisorb CO_2. This result makes sense chemically since adsorption of CO_2 on basic solids forms surface carbonate structures that can be easily identified by infrared spectroscopy. The CO_2 adsorbs most favorably at the Cs–O pair present at the low index surface plane. The adsorption is quite strong at -284 kJ mol^{-1}, presumably because of the basicity of the oxide surface and the multidentate nature of the adsorbate structure. It is interesting to note that the bind-

ing energy from our calculation is similar to that obtained by adsorption microcalorimetry on bulk "Cs_2O" obtained from Aldrich (see Fig. 5). Even though bulk "Cs_2O" is a mixture of peroxide and superoxide, it is quite possible that the oxide surface restructures under vacuum treatment at 623 K in the microcalorimeter to reveal a Cs_2O-like configuration. More importantly, the low heat of CO_2 adsorption on zeolite supported cesium oxide (-100 kJ mol^{-1}) suggests that the oxide clusters are not stoichiometric oxides.

We next explored the adsorption of CO_2 on model Cs_2O_2 surfaces. The calculated adsorption energy for unidentate CO_2 on the (001) surface of Cs_2O_2 was -95 kJ mol^{-1}, which is much closer to the adsorption energy found on zeolite-supported cesium oxide. Analogous calculations on the bidentate structures (see Fig. 6) indicated that bidentate adsorption was favored over unidentate adsorption. In addition, the binding energy varied from -124 to -186 kJ mol^{-1}, depending on the exposed crystal plane. Nevertheless, the binding energy of the configurations we explored on Cs_2O_2 were always significantly less than that on stoichiometric Cs_2O and was closer to the enthalpies of adsorption measured in our microcalorimeter for CO_2 adsorbing on zeolite-supported cesium oxide. Attempts to adsorb CO_2 onto a model surface of CsO_2 were unsuccessful. The oxygen-rich surface repels the carbon dioxide.

Two important trends were observed in this study. First, the adsorption strength of CO_2 on cesium oxides increased in the order $CsO_2 < Cs_2O_2 < Cs_2O$, which parallels the anticipated order in basicity. Second, the calculated values of binding energy suggest that cesium oxide occluded into zeolite pores is not a stoichiometric oxide as proposed by many researchers, but may instead be a peroxide. Indeed, our measured stoichiometry of adsorption (1 CO_2 adsorbed per 4 occluded Cs atoms) does not match that needed to convert stoichiometric Cs_2O into Cs_2CO_3. Much additional work is needed to clarify these issues. For example, the stability and basicity of stoichiometric oxide and peroxide nanoclusters need to be elucidated. In addition, the role of the zeolite support on the structure and basicity of the occluded oxides should be explored.

5. Catalytic activity of occluded cesium oxide clusters

The rather moderate adsorption strength of CO_2 on zeolites containing occluded alkali metal oxides suggests that CO_2 can be used as a reagent in a catalytic reaction on these solids. Cyclic carbonates synthesized by the addition of CO_2 to epoxides are useful as highly polar solvents and reagents in polymer synthesis [66–70]. Many organic and inorganic compounds, including onium halides, phosphines, amines, and metal halides, catalyze the reaction of CO_2 with epoxides under mild conditions to give high yields of cyclic carbonate [66–68]. Solid bases such as MgO and calcined hydrotalcite (Mg–Al mixed oxide) have also been explored as possible catalysts for the reaction [69,70]. Interestingly, stereospecific addition of CO_2 has been reported over the Mg-based solid oxides.

We investigated the reactions of CO_2 with ethylene oxide and epoxypropylbenzene over a series of base catalysts, including alkali-loaded X zeolites, Cs-loaded alumina, and magnesia, as well as a homogeneous catalyst, tetraethylammonium bromide [71]. To make the comparison between homogeneous and heterogeneous catalysis, rates on the zeolites were expressed as site–time yields based on active sites counted by CO_2 adsorption, whereas the rates with $[N(C_2H_5)_4]Br$ were based on the number of formula units. Interestingly, the homogeneous catalyst was only 3 to 4 times more active for the cycloaddition of CO_2 to ethylene oxide than the basic zeolite catalysts containing occluded alkali metal oxide.

The reactivity results also indicated that basicity affects the rate of cycloaddition of carbon dioxide to epoxides [71]. For example, the rate of ethylene carbonate formation over basic zeolites increased with increasing basicity as evaluated by carbon dioxide adsorption microcalorimetry. Clearly, the basic strength of a catalyst cannot be too great or carbon dioxide will be adsorbed too strongly to react. The catalysts used in this study are apparently of appropriate base strength to allows both CO_2 adsorption and subsequent reaction.

Although epoxypropylbenzene and ethylene oxide reacted at about the same rate (within about a factor of 3) in the presence of a homogeneous catalyst, the larger epoxide reacted an order of magnitude slower than the smaller one on the solid catalysts. Apparently, the steric restrictions caused by the bulky substituent lowered the observed rate of epoxypropylbenzene conversion on solid catalyst surfaces. Rates of reaction with mixed epoxides (both epoxypropylbenzene and ethylene oxide in the reactor) were consistent with the majority of active sites on the zeolites being located in the micropores instead of on the external surface. This phenomenon of "reverse" reactant shape selectivity is illustrated in Fig. 7. For the mixed epoxide experiments, both epoxypropylbenzene and its cyclic carbonate retarded the diffusion of ethylene oxide into the zeolite pores and severely reduced the production of ethylene carbonate. However, the bulky reactant and product negligibly affected the rate of ethylene carbonate production over nonmicroporous MgO. These results indicate that most of the basic sites of the zeolite catalysts containing occluded alkali metal oxide species are within the micropore network and suggest their use as shape-selective base catalysts. Indeed, future work with these materials should exploit the molecular sieving property of the zeolite support.

It has been reported that the calcined hydrotalcite (Mg–Al mixed oxide) was more active than MgO in the reaction of CO_2 with epoxides because of the coexistence of Lewis acid sites on the former [70]. These acid sites are believed to stabilize the adsorbed epoxide prior to addition of carbon dioxide. Therefore, the proximity of Lewis acid sites to basic sites capable of adsorbing carbon dioxide may be required to catalyze the cycloaddition reaction. A possible

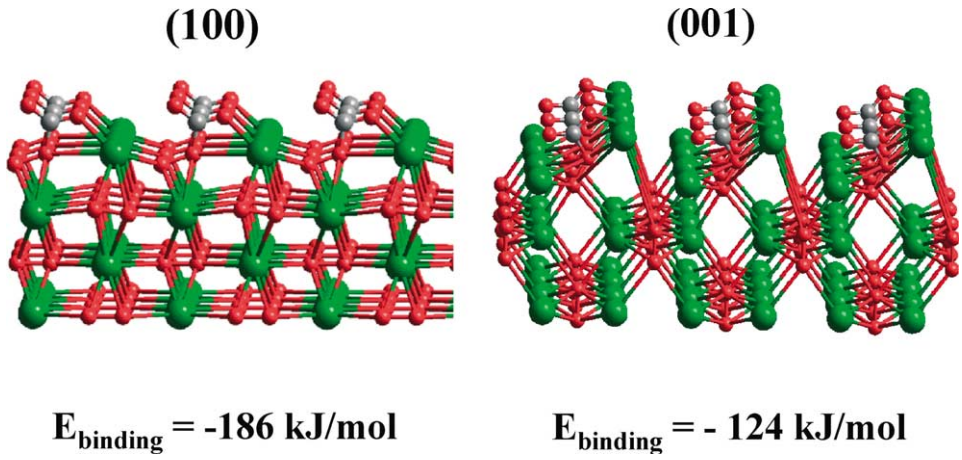

Fig. 6. Adsorption of CO_2 in bidentate mode on low index planes of Cs_2O_2. The (001) plane undergoes significant reconstruction upon adsorption. The largest spheres represent cesium atoms and the smallest spheres represent oxygen atoms. Other spheres represent carbon atoms.

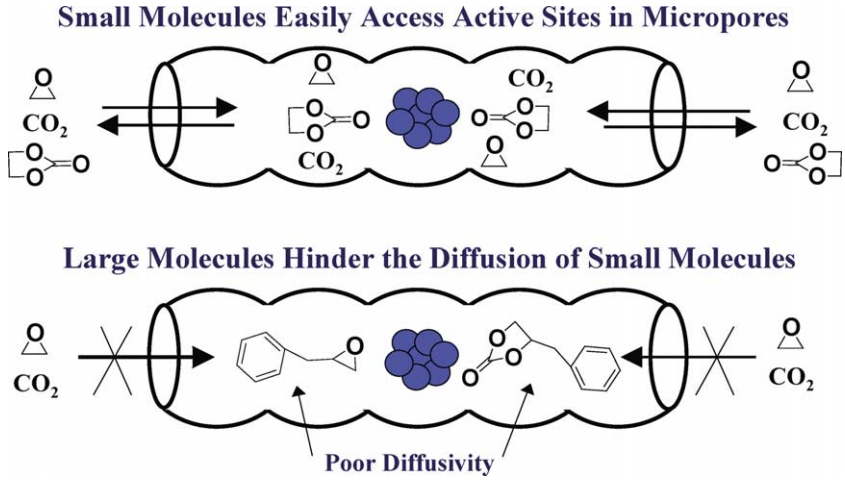

Fig. 7. Schematic illustration of how the bulky epoxide (epoxypropylbenzene) in a microporous base catalyst inhibits the reaction of ethylene oxide with CO_2 to form ethylene carbonate.

reaction mechanism for the addition of CO_2 to epoxides over solid base catalysts has been suggested by Yamaguchi et al. [70]. In that mechanism, carbon dioxide is adsorbed on Lewis base sites (e.g., O^{2-}) to form a surface carbonate species. The strength and number of the surface base sites are likely to be very important for the activation of CO_2. The epoxide is then adsorbed onto a neighboring Lewis acid site, most likely an exposed cation. The carbonate surface anion reacts with the less sterically hindered carbon atom of the adsorbed oxirane to generate the oxy anion, which subsequently yields the cyclic carbonate product. For the basic zeolites, the exchangeable cations provide adequate coordination sites for the reacting epoxides. Similarly to the case of toluene alkylation with methanol, neighboring Lewis *acid* and *base* sites are apparently needed for the reaction to occur. The well-known idea of acid–base bifunctionality in zeolite catalysts applies to this case.

Although results from CO_2 adsorption microcalorimetry indicate that the majority of base sites on CsO_x/CsX are not very strong, this material catalyzes double bond shift in

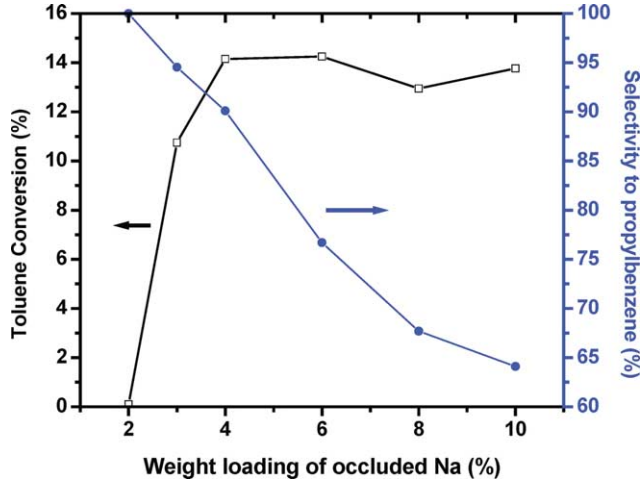

Fig. 8. Effect of Na azide loading on NaX zeolite for side-chain alkylation of toluene with ethylene at 523 K. The major products are from mono-, di-, and tri-alkylation reactions. Selectivity refers to the amount of mono-alkylated product formed relative to all alkylation products. (Adapted from J. Tai, MS thesis, University of Virginia, 2001.)

olefins at relatively low temperature [5,58,64]. For example, the isomerization of 1-butene to *cis*- and *trans*-2-butene is catalyzed with high rate and selectivity to the *cis* product at 373 K. To help quantify the number of active sites for butene isomerization, CO_2 poisoning experiments were performed [72]. In this set of experiments, a pretreated catalyst was purposefully exposed to a known amount of CO_2 to eliminate all activity. Then the catalyst was thermally treated in helium at various temperatures to desorb the adsorbed CO_2. Isomerization rates were measured after each activation step. For CsO_x/CsX, virtually no activity was observed after treatments at 373, 473, and 573 K. The catalyst recovered about 20% of the original activity after treatment in He at 673 K for 2 h and was completely regenerated after heating at 773 K for 2 h. These observations demonstrate that the active sites in 1-butene isomerization are mainly those associated with a CO_2 desorption temperature greater than 673 K, which are only about 5% of the entire CO_2 inventory adsorbed on CsO_x/CsX at 373 K. The atomic structure of these few active sites on zeolite catalysts is currently unknown but is the subject of on-going investigation.

6. Basic zeolites containing occluded alkali metals

Zeolites containing alkali metals in cages have been investigated as high-strength solid base catalysts. A novel preparation technique has been reported in which alkali metal clusters are prepared via the decomposition of alkali metal azides in the presence of a zeolite [73–81]. Unlike their alkali metal counterparts, the azides themselves are stable at ambient conditions. Decomposition of the alkali azide in the pores of the zeolite has been claimed to form either ionic or neutral alkali metal clusters, depending primarily on the heating rate used to decompose the supported azide; faster heating rates ($\sim 25\ \mathrm{K\,min^{-1}}$) resulted in ionic clusters while slower heating rates ($\sim 1\ \mathrm{K\,min^{-1}}$) gave primarily neutral metal clusters [80]. Electron spin resonance (ESR) spectroscopy was used to determine whether alkali metal or ionic clusters were present in the cages of X and Y zeolites [75,80,82]. Interestingly, charged alkali metal clusters of Na and K (i.e., Na_4^{3+}, Na_3^{2+}, Na_2^{+}, K_3^{2+}) were also observed by ESR spectroscopy of ion-exchanged zeolites after irradiation by γ-rays [83–87]. Neutral alkali metal clusters were not reported in the studies involving irradiation of zeolites. Although some of the clusters formed by decomposition of alkali metal azides in zeolites are claimed to be neutral, it is likely that some charge is associated with the cluster due to the interaction with the support. In the following paragraphs, the term alkali metal cluster refers to a product of azide decomposition having an undetermined charge.

We have also used ESR spectroscopy to characterize zeolites that have been loaded with alkali metal azide and thermally treated [88]. For example, the location of the central line g-value in the ESR spectrum of the alkali-metal-loaded KX zeolites indicated the formation of potassium clusters, despite the use of sodium and cesium azides as precursors. Xu and Kevan [74] also reported this result for NaN_3 and CsN_3 decomposed on KX zeolite. Apparently, the zeolite cations exchanged with the impregnated alkali either during azide impregnation or thermal treatment. Reduction of potassium ions by cesium metal makes sense thermodynamically, but reduction of potassium ions by sodium metal is harder to rationalize. Evidently, the reduction potential of a cluster of potassium cations in a zeolite host is sufficiently different than that of a bare cation to enable electron transfer from the added Na. The dehydrated zeolite plays the role of a polar solid solvent in this reduction reaction [89]. Interestingly, both of the KX zeolites also exhibited broad ESR lines at high g-values, indicating the presence of additional extralattice alkali metal clusters. The relative importance of extraframework metal clusters in catalytic reactions is discussed in the next section.

7. Reactions on zeolite-supported alkali metals

The side-chain alkylation of aromatics with olefins is catalyzed by strong solid bases like alkali metals. Pines and co-workers did pioneering work on the side-chain alkylation of alkylbenzenes with olefins [90–92]. They carried out the reaction using sodium metal in the presence of organic promoters such as anthracene, *o*-chlorotoluene, *o*-toluic acid, pyridine, and organic peroxides. The sodium metal reacted in situ with the organic promoter to form an organosodium compound, which then catalyzed the alkylation reaction. Martens et al. have studied the side-chain alkylation of alkylaromatics with ethylene over zeolites containing occluded alkali metals [93]. They observed that the alkylation activity of Na metal in NaX zeolite was higher than that of Na metal in NaY zeolite. Also, the alkylation activity for isopropylbenzene was lower than that of ethylbenzene, possibly due to steric effects.

We have investigated the influence of azide loading on the side-chain alkylation of toluene with ethylene [94]. Figure 8 summarizes the results from that study. At very low loadings (< 2 wt% Na), the catalysts were essentially inactive in the reaction. At higher loadings (> 6%), the conversion of toluene was essentially constant at about 14% whereas the selectivity to monoalkylated product continually decreased. Evidently, higher loadings of azide precursor eventually form catalysts with a propensity for di- and tri-side-chain alkylation of toluene with ethylene. We speculate that Na "metal" clusters are ultimately deposited on the external surfaces of the zeolite at higher loadings. Thus, the shape-selective environment of the supercage, which minimizes multiple side-chain alkylation reactions, is no longer important at the higher loadings.

We also investigated the liquid-phase side-chain alkenylation reaction of *o*-xylene with butadiene to form 5-*o*-tolyl-2-pentene, or OTP [88]. Like side-chain alkylation of toluene with ethylene, the side-chain alkenylation re-

action requires a base site stronger than that associated with supported alkali metal oxides. The selectivity to OTP, based on the total amount of mono-, di-, and tri-side-chain-alkenylated products, was greater than 85% for *o*-xylene conversions ranging from 1 to 14%. The active materials were true catalysts since the ratio of the amount of *o*-xylene reacted to the theoretical amount of alkali metal present exceeded unity after a reaction time of 7.5 h. The OTP product formed over Cs/KX had a *trans*/*cis* ratio of 1.3, which was close to that seen over unsupported potassium metal, which according to ESR spectroscopy was present in the zeolite cages.

Extralattice metal clusters were evident on each of the alkali-metal-loaded zeolites, which were effective catalysts for the side-chain alkenylation reaction, suggesting that these clusters might be the active species. For each reaction in which OTP was produced, the solution color indicated that alkali metal formed from the decomposition of the supported azide may have leached into solution to form an organoalkali complex. Thus, catalytic activity was likely due to metal species in the solution as well as those associated with the zeolite (possibly through reaction with the zeolite).

The difficulty with maintaining the "metal" phase inside the microporous environment and the extreme sensitivity of these alkali metals to poisons limit their usefulness. However, if these major problems can be overcome, these materials are potentially useful strong base shape-selective catalysts. One can envision that the microporous environment inside a zeolite might even prevent or slow deactivation of the alkali metal during catalytic reaction if oligomerization side reactions are responsible for the loss in activity. The steric restrictions in the micropore should prevent bimolecular reactions involving large molecules.

8. Basic zeolites as supports for transition metals

Base-promoted Ru materials are expected to become the second-generation ammonia synthesis catalyst since they permit milder operating conditions than the conventional Fe-based catalyst [95,96]. Zeolites are of particular interest as supports for Ru since the maximum size of occluded metal particles is limited to the size of the zeolite pores or cages. Also, the basicity of the zeolite is easily modified by ion exchange with Group IA and IIA cations, with the consensus being the promoter effectiveness for supported ruthenium catalysts increases with basicity.

Cisneros and Lunsford studied ammonia synthesis catalyzed by ruthenium supported on alkali-metal-exchanged zeolites X and Y [97]. The catalysts were found to be active at atmospheric pressure over the temperature range from 573 to 723 K, with ruthenium-supported zeolite X being more effective. They found the activity to be strongly dependent on the zeolite cations, the turnover frequency increasing in the order Cs < Na < K for ion-exchanged X zeolites. The turnover frequency was a factor of 25 less over Ru/CsX compared to Ru/KX at 350 °C, presumably due to the relatively low level of Cs exchange in their sample. Cisneros and Lunsford concluded that the turnover frequency decreased as the partial charge of the zeolite support increased by changing the alkali compensating cation. Our lab found that CsX was a better support than KX for a Ru ammonia catalyst, which agrees with basicity ranking of the zeolites [98].

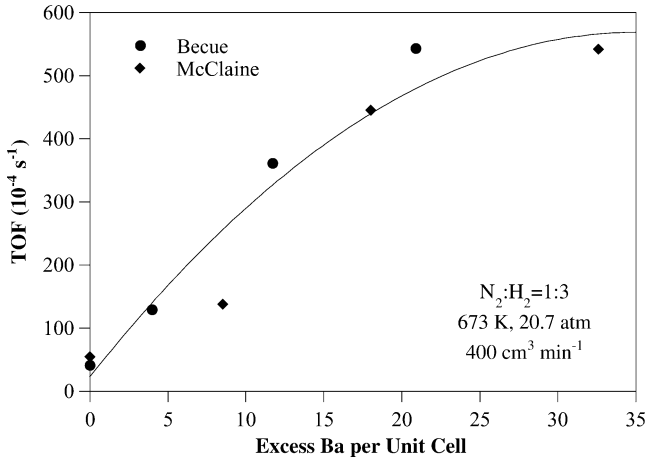

Fig. 9. Effect of added barium on ammonia synthesis turnover frequency over Ru/BaX at constant ammonia pressure (0.001 atm). The two different symbols represent results from two different catalyst batches prepared and tested by two different people. (Adapted from B.C. McClaine, T. Becue, C. Lock, R.J. Davis, Kinetic Analysis of Ammonia Synthesis Catalyzed by Barium-Promoted Ruthenium Supported on Zeolite X, J. Mol. Catal. A Chem. 163 (2000) 105–116, with permission from Elsevier Science.)

We have also synthesized nanometer-sized Ru metal clusters inside the cages of KX and BaX zeolite and subsequently promoted the catalyst with occluded K and Ba compounds, respectively [99]. The promotional effect of Ba on Ru-catalyzed ammonia synthesis at 20.7 atm was superior to that of K, which is counter to the anticipated basicity of the occluded compounds. More importantly, addition of Ba beyond ion-exchange capacity promoted the reaction on intrazeolitic Ru by an order of magnitude, as illustrated in Fig. 9 [99,100].

Analysis of Ru *K*-edge EXAFS recorded at low temperatures in H_2 indicated that the zeolite-supported Ru clusters were about 1 nm in diameter, regardless of barium loading [101]. The average Ru–Ru coordination number was 4.8 at an interatomic distance of 2.61 Å. Adding barium to Ru/BaX beyond ion-exchange capacity caused new features to appear in the Ru EXAFS that were attributed to the interaction of oxygen atoms with Ru clusters at a distance of 1.91 Å. It should be noted that a short Ru–Ba distance of about 2 Å can also fit the EXAFS spectrum. The combination of infrared and Ba L_{III} near-edge spectroscopy revealed that the occluded barium was predominantly in a carbonate form prior to treatment in dihydrogen, but most of this carbonate decomposed after heating to 773 K in H_2. Since incorporation of Ba into the samples did not alter the structure or chemical state of the Ru clusters, the promotional effect

Table 1
Results from isotopic transient analysis of Ru catalysts for ammonia synthesis[a]

	τ[b] (s)	Fractional[c] coverage	Turnover frequency[d] (s^{-1})
Ru/SiO_2	670	0.030	0.0015
Ba–Ru/BaX	15	0.064	0.0670
Cs–Ru/MgO	7.1	0.051	0.1410

[a] Stoichiometric feed at 3 atm total pressure and 673 K [102].
[b] The average residence time of nitrogen-containing intermediates on the surface.
[c] The fractional coverage of the Ru surface by nitrogen-containing intermediates.
[d] Inverse of τ.

of Ba on ammonia synthesis rate is likely due to the creation of highly active sites at the promoter–metal interface.

Steady-state isotopic transient kinetic analysis was used to evaluate the intrinsic turnover frequency (TOF_{intr}) and the fractional surface coverage of nitrogen-containing species (θ_{NH_x}) on a Ba-promoted Ru/BaX zeolite catalyst during ammonia synthesis at 3 atm, 673 K, and a stoichiometric ratio of N_2 and H_2 [102]. In the case of the basic zeolite catalyst, artifacts resulting from inter- and intraparticle readsorption of product ammonia on the kinetic parameters were removed by co-feeding ammonia to the system and varying the total flow rate. The values of TOF_{intr} and θ_{NH_x} determined from the intrinsic lifetime of surface intermediates at low ammonia pressure were 0.067 s^{-1} and 0.064, respectively. In Table 1, parameters for the zeolite-supported catalyst are compared to those of a poorly active, unpromoted Ru/SiO_2 catalyst and a highly active Cs-promoted Ru/MgO catalyst. Although the TOF_{intr} spanned two orders of magnitude, the value of θ_{NH_x} was very low and fairly independent of support and/or promoter. From these results, it appears that base promoters increase the intrinsic turnover frequency of the active Ru sites by an electronic effect that lowers the barrier for N_2 dissociation (the rate-determining step) since the surface coverage of nitrogen-containing intermediates was about the same for all of the catalysts. These results also show that basic zeolites can function as very effective supports for transition metals.

9. Summary

Zeolite X is a microporous aluminosilicate having a silicon-to-aluminum ratio ranging from 1 to 1.5. Because of the significant negative framework charge of zeolite X, it functions as an effective electron donor, especially when a heavy alkali metal cation such as Cs^+ is present for electroneutrality. Although alkali-exchanged zeolites are considered to be solid base catalysts for the alkylation of toluene with methanol, the active site should be envisioned as a combination of a Lewis acid and a Lewis base site.

Additional base sites can be formed in zeolite X by decomposition of supported alkali metal precursors into occluded oxides. However, the resulting materials do not appear to be as strong as bulk phase alkali metal oxides and may actually be peroxides instead, depending on the conditions of pretreatment. Cycloaddition of CO_2 to ethylene oxide is catalyzed by alkali metal oxides occluded in zeolite micropores at nearly the same rate (within about a factor of 3) as a homogeneous catalyst, demonstrating the similarity between homogeneous and heterogeneous base catalysis for this case. Analogous to toluene alkylation with methanol over ion-exchanged zeolites, Lewis acid–base pairs are likely to be important for the cycloaddition of CO_2 to epoxides.

Incorporation of alkali metals into zeolite X via decomposition of the corresponding azide results in the formation of very strong bases capable of catalyzing toluene alkylation with ethylene. However, extreme sensitivity of these materials to poisons and migration of the metal to the external surface currently limit their utility.

Basic zeolites are also excellent supports for a transition metal like Ru, which is considered to be the active component of a second-generation ammonia synthesis catalyst. In that system, Ba-exchanged X zeolite that contains 1-nm Ru metal clusters is promoted by occluded BaO for the synthesis of ammonia. Presumably, interfacial contact of Ru active sites with basic BaO promotes the dissociation of N_2, the rate-determining step.

These examples illustrate the wide utility and untapped potential of basic zeolites as catalysts and catalyst supports.

Acknowledgments

R.J.D. acknowledges the many graduate students, postdoctoral researchers, and collaborators who worked on basic zeolites in his laboratory. This work is currently supported by the Department of Energy—Basic Energy Sciences (DEFG02-95ER14549) and the National Science Foundation (CTS-9729812).

References

[1] K. Tanabe, W.F. Holderich, Appl. Catal. A Gen. 181 (1999) 399.
[2] C.B. Dartt, M.E. Davis, Catal. Today 19 (1994) 151.
[3] G.C. Tustin, M. Rule, J. Catal. 147 (1994) 186.
[4] D. Barthomeuf, Catal. Rev. Sci. Eng. 38 (1996) 521.
[5] H. Tsuji, F. Yagi, H. Hattori, H. Kita, Stud. Surf. Sci. Catal. 75 (1992) 1171.
[6] P.A. Jacobs, F.H. van Cauwelaert, E.F. Vansant, J.B. Uytterhoeven, J. Chem. Soc. Faraday Trans. 1 69 (1973) 1056.
[7] P.A. Jacobs, F.H. van Cauwelaert, E.F. Vansant, J. Chem. Soc. Faraday Trans. 1 69 (1973) 2130.
[8] A.A. Davydov, M.L. Shepot'ko, A.A. Budneva, Kinet. Katal. 35 (1994) 299.
[9] F. Yagi, H. Tsuji, H. Hattori, Micropor. Mater. 9 (1997) 237.
[10] J.C. Lavalley, Catal. Today 27 (1996) 377.
[11] M. Huang, S. Kaliaguine, J. Chem. Soc. Faraday Trans. 88 (1992) 751.
[12] D. Murphy, P. Massiani, R. Franck, D. Barthomeuf, J. Phys. Chem. 100 (1996) 6731.
[13] T.A. Gordymova, A.A. Davydov, React. Kinet. Catal. Lett. 23 (1983) 233.

[14] E.B. Uvarova, L.M. Kustov, V.B. Kazansky, Stud. Surf. Sci. Catal. 94 (1995) 254.
[15] J. Xie, M. Huang, S. Kaliaguine, React. Kinet. Catal. Lett. 58 (1996) 217.
[16] S.H. Hastings, J.L. Franklin, J.C. Schiller, F.A. Matsen, J. Am. Chem. Soc. 75 (1953) 2900.
[17] F.T. Lang, R.L. Strong, J. Am. Chem. Soc. 87 (1965) 2345.
[18] E.I. Ginns, R.L. Strong, J. Phys. Chem. 71 (1967) 3059.
[19] M. Tamres, S.N. Bhat, J. Phys. Chem. 75 (1971) 1057.
[20] J. Grundnes, M. Tamres, S.N. Bhat, J. Phys. Chem. 75 (1971) 3682.
[21] M. Tamres, S.N. Bhat, J. Am. Chem. Soc. 94 (1972) 2577.
[22] M. Tamres, S.N. Bhat, J. Am. Chem. Soc. 95 (1973) 2516.
[23] H.A. Benesi, J.H. Hildebrand, J. Am. Chem. Soc. 71 (1949) 2703.
[24] R.S. Mulliken, J. Am. Chem. Soc. 74 (1952) 811.
[25] J. Ham, J. Am. Chem. Soc. 76 (1954) 3875.
[26] S. Nagakura, J. Am. Chem. Soc. 80 (1958) 520.
[27] J. Walkley, D.N. Glew, J.H. Hildebrand, J. Chem. Phys. 72 (1960) 621.
[28] S.M. Brandon, M. Tamres, S. Searles Jr., J. Am. Chem. Soc. 82 (1960) 2129.
[29] R.P. Lang, J. Am. Chem. Soc. 84 (1962) 1185.
[30] T. Kubota, J. Am. Chem. Soc. 87 (1965) 458.
[31] J.H. Hildebrand, Science 150 (1965) 441.
[32] E.M. Voigt, J. Phys. Chem. 72 (1968) 3300.
[33] S. Sawamura, Y. Taniguchi, K. Suzuki, Bull. Chem. Soc. Jpn. 52 (1979) 3511.
[34] V.P. Shedbalkar, S.N. Bhat, Ind. J. Chem. A 22 (1983) 318.
[35] V.P. Shedbalkar, S.N. Bhat, Ind. J. Chem. A 22 (1983) 1062.
[36] G.V. Belysheva, O.N. Karpov, M.A. Lopatin, P.G. Sennikov, A.N. Egorochikin, Izv. Akad. Nauk SSSR Ser. Khim. 7 (1990) 1574.
[37] G.B. Rao, N.S. Rao, Spectrochim. Acta Part A 46 (1990) 1107.
[38] M. Tamres, D.R. Virzi, S. Searles, J. Am. Chem. Soc. 75 (1953) 4358.
[39] R.M. Barrer, S. Wasilewski, Trans. Faraday Soc. 57 (1961) 1140.
[40] K. Seff, D.P. Shoemaker, Acta Crystallogr. 22 (1967) 162.
[41] S.Y. Choi, Y.S. Park, S.B. Hong, K.B. Yoon, J. Am. Chem. Soc. 118 (1996) 9377.
[42] E.J. Doskocil, S.V. Bordawekar, B.G. Kaye, R.J. Davis, J. Phys. Chem. B 103 (1999) 6277.
[43] X. Liu, K.-K. Iu, J.K. Thomas, J. Phys. Chem. 98 (1994) 7877.
[44] X. Liu, K.-K. Iu, J.K. Thomas, Chem. Phys. Lett. 204 (1993) 163.
[45] S. Hashimoto, J. Chem. Soc. Faraday Trans. 93 (1997) 4401.
[46] Y.S. Park, S.Y. Um, K.B. Yoon, J. Am. Chem. Soc. 121 (1999) 3193.
[47] H.J.D. McManus, C. Finel, L. Kevan, Radiat. Phys. Chem. 45 (1995) 761.
[48] M. Alvaro, H. Garcia, S. Garcia, F. Marquez, J.C. Scaiano, J. Phys. Chem. B 101 (1997) 3043.
[49] J.K. Thomas, Chem. Rev. 93 (1993) 301.
[50] T. Yashima, K. Sato, T. Hayasaka, N. Hara, J. Catal. 26 (1972) 303.
[51] W.S. Wieland, R.J. Davis, J.M. Garces, Catal. Today 28 (1996) 443.
[52] W.S. Wieland, R.J. Davis, J.M. Garces, J. Catal. 173 (1998) 490.
[53] A.E. Palomeres, G. Eder-Mirth, M. Rep, J.A. Lercher, J. Catal. 180 (1998) 56.
[54] E.J. Lee, Y.S. Park, K.B. Yoon, Chem. Commun. (2001) 1882.
[55] P.E. Hathaway, M.E. Davis, J. Catal. 116 (1989) 263.
[56] H. Tsuji, F. Yagi, H. Hattori, Chem. Lett. (1991) 1881.
[57] I. Rodriguez, H. Cambon, D. Brunel, M. Lasperas, P. Geneste, Stud. Surf. Sci. Catal. 78 (1993) 623.
[58] J.C. Kim, H.-X. Li, C.-Y. Chen, M.E. Davis, Micropor. Mater. 2 (1994) 413.
[59] M. Lasperas, H. Cambon, D. Brunel, I. Rodriguez, P. Geneste, Micropor. Mater. 7 (1996) 61.
[60] I. Rodriguez, H. Cambon, D. Brunel, M. Lasperas, J. Mol. Catal. A Chem. 130 (1998) 195.
[61] F. Yagi, N. Kanuka, H. Tsuji, S. Nakata, H. Kita, H. Hattori, Micropor. Mater. 9 (1997) 229.
[62] M. Hunger, U. Schenk, B. Burger, J. Weitkamp, Angew. Chem. Int. Ed. Engl. 36 (1997) 2504.
[63] T.R. Krawietz, D.K. Murray, J.F. Haw, J. Phys. Chem. A 102 (1998) 8779.
[64] S.V. Bordawekar, R.J. Davis, J. Catal. 189 (2000) 79.
[65] J. Tai, Q. Ge, R.J. Davis, M. Neurock, to be submitted.
[66] D.J. Darensbourg, M.W. Holtcamp, Coord. Chem. Rev. 153 (1996) 155.
[67] M. Lichtenwalter, J.F. Cooper, US Patent 2,773,070, 1956, assigned to Jefferson Chemical Co.;
P.P. McClellan, US Patent 2,873,282, 1959, assigned to Jefferson Chemical Co.;
C.H. McMullen, J.R. Nelson, B.C. Ream, J.A. Sims, UK Patent 2,011,402A, 1978, assigned to Union Carbide Corp.
[68] N.H. Kihara, T. Endo, J. Org. Chem. 58 (1993) 6198.
[69] T. Yano, H. Matsui, T. Koike, H. Ishiguro, H. Fujihara, M. Yoshihara, T. Maeshima, Chem. Commun. (1997) 1129.
[70] K. Yamaguchi, K. Ebitani, T. Yoshida, H. Yoshida, K. Kaneda, J. Am. Chem. Soc. 121 (1999) 4526.
[71] M. Tu, R.J. Davis, J. Catal. 199 (2001) 85.
[72] J. Li, R.J. Davis, Appl. Catal. A Gen., in press.
[73] B. Xu, L. Kevan, J. Chem. Soc. Faraday Trans. 87 (1991) 2843.
[74] B. Xu, L. Kevan, J. Phys. Chem. 96 (1992) 2642.
[75] B. Xu, X. Chen, L. Kevan, J. Chem. Soc. Faraday Trans. 87 (1991) 3157.
[76] M. Brock, C. Edwards, H. Förster, M. Schröder, Stud. Surf. Sci. Catal. 84 (1994) 1515.
[77] I. Hannus, I. Kiricsi, A. Beres, J.B. Nagy, H. Forster, Stud. Surf. Sci. Catal. 98 (1995) 81.
[78] A. Beres, I. Hannus, I. Kiricsi, J. Therm. Anal. 46 (1996) 1301.
[79] L.R.M. Martens, P.J. Grobet, P.A. Jacobs, Nature 315 (1985) 568.
[80] L.R.M. Martens, P.J. Grobet, W.J.M. Vermeiren, P.A. Jacobs, Stud. Surf. Sci. Catal. 28 (1986) 935.
[81] A. Beres, I. Hannus, I. Kiricsi, J. Therm. Anal. 47 (1996) 419.
[82] Y.S. Park, Y.S. Lee, K.B. Yoon, Stud. Surf. Sci. Catal. 84 (1994) 901.
[83] K.-K. Iu, X. Liu, J.K. Thomas, J. Phys. Chem. 97 (1993) 8165.
[84] X. Liu, J.K. Thomas, Chem. Phys. Lett. 192 (1992) 555.
[85] X. Liu, J.K. Thomas, Langmuir 8 (1992) 1750.
[86] X. Liu, G. Zhang, J.K. Thomas, J. Phys. Chem. 99 (1995) 10024.
[87] X. Liu, K.-K. Iu, J.K. Thomas, J. Phys. Chem. 98 (1994) 13720.
[88] E.J. Doskocil, R.J. Davis, J. Catal. 188 (1999) 353.
[89] P.P. Edwards, P.A. Anderson, J.M. Thomas, Acc. Chem. Res. 29 (1996) 23.
[90] H. Pines, J.A. Vesely, V.N. Ipatieff, J. Am. Chem. Soc. 77 (1955) 554.
[91] H. Pines, V. Mark, J. Am. Chem. Soc. 78 (1956) 4316.
[92] H. Pines, L. Schaap, J. Am. Chem. Soc. 80 (1958) 3076.
[93] L.R. Martens, W.J. Vermeiren, D.R. Huybrechts, P.J. Grobet, P.A. Jacobs, in: M.J. Phillips, M. Ternan (Eds.), Proceedings of the 9th International Congress on Catalysis, Chem. Institute of Canada, Ottawa, 1988, p. 420.
[94] J. Tai, Side chain alkylation of toluene catalyzed by alkali metal azides supported on basic oxides, MS thesis, University of Virginia, 2001.
[95] A. Ozaki, K.-I. Aika, A. Furata, A. Okagami, US Patent 3,770,658, 1973.
[96] K.-I. Aika, H. Hori, A. Tamaru, J. Catal. 27 (1972) 424.
[97] M.D. Cisneros, J.H. Lunsford, J. Catal. 141 (1993) 191.
[98] C.T. Fishel, R.J. Davis, J.M. Garces, J. Catal. 163 (1996) 148.
[99] T. Becue, R.J. Davis, J.M. Garces, J. Catal. 179 (1998) 129.
[100] B.C. McClaine, T. Becue, C. Lock, R.J. Davis, J. Mol. Catal. A Chem. 163 (2000) 105.
[101] B.C. McClaine, S.E. Siporin, R.J. Davis, J. Phys. Chem. B 105 (2001) 7525.
[102] B.C. McClaine, R.J. Davis, J. Catal. 211 (2002) 379.